

Sonoelectroanalysis: A Review

by **Craig E. Banks and Richard G. Compton***

*Physical and Theoretical Chemistry Laboratory, University of Oxford,
South Parks Road, Oxford, OX1 3QZ, United Kingdom*

Key words: sonoelectroanalysis, ultrasound, electrochemistry

This review highlights recent advances made towards improving sonoelectroanalysis with an emphasis on applications where conventional electrochemical methodologies often fail. It is shown that: 1) the significantly increased mass transport regime under insonation very considerably enhances the sensitivity in comparison to what would be obtained under quiescent conditions and, in particular, 2) cavitation activity at the electrode solution interface provides depassivation in highly 'dirty' media or in the presence of undesirable surface active species and so can preserve quantitative electrode activity in complex, real world samples so removing the requirements for sample pretreatment which has hitherto limited the wider applications, for example, of stripping voltammetry.

W pracy przedstawiono ostatnie osiągnięcia w elektroanalizie z użyciem ultradźwięków. Szczególny nacisk położono na te zastosowania, w których tradycyjne postępowanie nie przynosi skutku. Pokazano, że: 1) napromieniowanie ultradźwiękami znacznie zwiększa szybkość transportu i czułość oznaczeń w porównaniu do spokojnych roztworów, i, w szczególności, 2) pojawiające się turbulencje dopasują elektrody w bardzo „zabrudzonych” środowiskach i w obecności niechcianych związków powierzchniowych, a tym samym przedłużają aktywność elektrod w złożonych rzeczywistych próbkach. Można wówczas zrezygnować ze wstępnego kondycjonowania elektrod i rozszerzyć pole zastosowań, np. w analizie strippingowej.

* Corresponding author. E-mail: Richard.Compton@chemistry.ox.ac.uk, Tel: 01865 275413. Fax: 01865 275410

The synergistic use of ultrasound with electrochemical processes, and electroanalytical procedures in particular has recently been found to be significantly beneficial. The purpose of this article is to summarise the known mechanisms by which ultrasound can influence an electrode processes and present some illustrations of the effectiveness of insonation in electroanalysis.

Power ultrasound is that within the frequency range 20 kHz and 100 kHz; these limits are usefully benchmarked against the sonic spectrum shown in Figure 1.

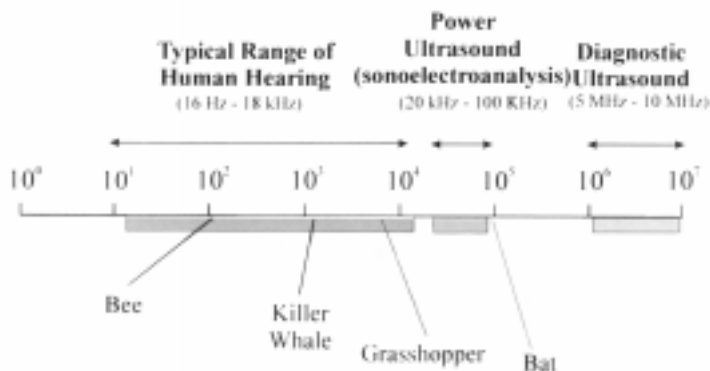


Figure 1. Ultrasonic spectrum detailing the range of ultrasonic frequencies

Note that the range of human hearing in healthy young adults at least, is from 16 Hz to 18 kHz [1]. High frequency ultrasound (1 MHz–10 MHz) is often applied in medical diagnosis but has found relatively little application in sonoelectrochemistry; rather almost all investigations have utilised power ultrasound (20–100 kHz). This is typically delivered to a fluid medium by means of a sonic horn such as is depicted in Figure 2.

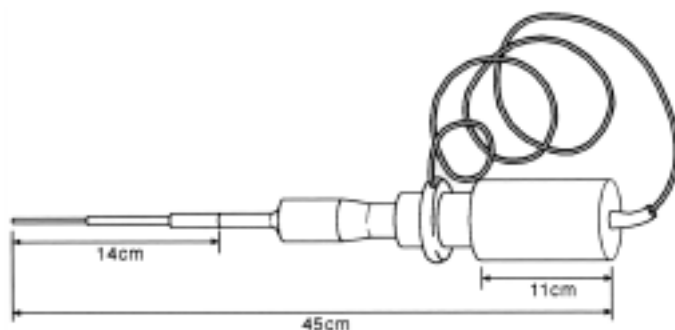


Figure 2. A commercial available ultrasonic horn available from a) Sonics & Materials, Inc. Newtown, CT 06470, U.S.A and b) Jencons -PLS, Bedfordshire, England

Immersion of the horn unit with a liquid leads to the efficient transmission of ultrasound. For electrochemistry two possible configurations offer themselves as summarised in Figure 3.

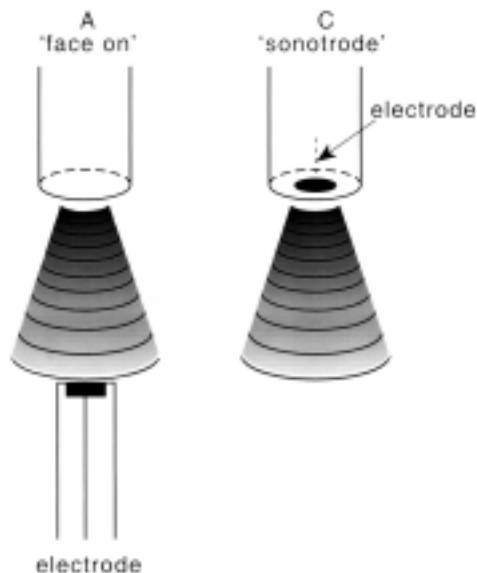


Figure 3. Electrode geometry's for sonoelectrochemistry

First is the 'face-on' mode [2–4] in which the horn is placed opposite to a working electrode in a conventional voltammetric cell. In this case an important variable is the electrode-to-horn separation (d) as well as the intensity of the ultrasound power. Alternatively a 'sonotrode' may be adopted: in this device [2,5–13] a single unit works both as the sonic transducer and as the working electrode. A simple schematic design is shown in Figure 4; refined versions are now available commercially.

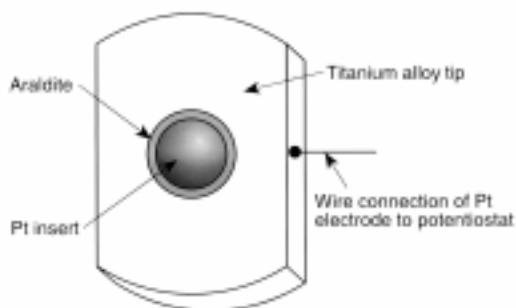


Figure 4. A schematic design of a sonotrode

Figure 5 shows typical contrasts between silent and sonovoltammetry. The data relates to the oxidation of ferrocene at a 2 mm platinum disc-electrode in acetonitrile containing 0.1 mol L^{-1} tetrabutylammonium perchlorate as supporting electrolyte and the insonation data has been obtained using a low power (50 W cm^{-2}) of ultrasound in a face-on mode with a horn to electrode separation of 4 mm. Notice that the familiar electrochemically reversible cyclic voltammogram seen under silent conditions is transformed into a hydrodynamic voltammogram with no forward/back sweep hysteresis. The voltammogram obtained under insonated conditions is significantly larger than the silent signal. In addition the limiting current is not flat as expected for a hydrodynamic voltammogram measured at a rotating disc electrode [14–18] or channel electrodes [19–31]. Rather there are irregular spikes present and the magnitudes of these are related to the power of the ultrasound applied.

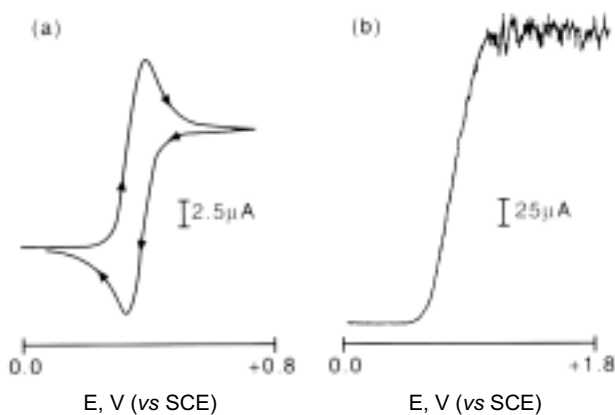


Figure 5. 2 mmol L^{-1} ferrocene in acetonitrile ($0.1 \text{ mol L}^{-1} \text{ NBu}_4\text{ClO}_4$) at a 2 mm diameter platinum electrode under silent conditions (a) and insonation of 50 W cm^{-2} (b), at a scan rate of 20 mV s^{-1} and a 40 mm electrode-horn separation

The voltammetric behaviour under insonation can be investigated by considering the modes of mass transport experienced by the electrode. Under silent conditions this is diffusion only whereas with insonation two new contributions arise (see Figure 6). The first is a strong turbulent convective flow, termed acoustic streaming [2,32–34] induced by the sonic horn in the fluid medium, and in which the average solution speed may be some tens of centimetres per second. Consequently an electrode located either close to (sonotrode) or below the horn tip experiences a substantial convective flow leading to the hydrodynamic nature of the voltammogram observed. In addition, beyond an ultrasound power threshold, cavitation (bubble formation) can occur [35–44], and this may occur preferentially on the electrode surface as compared to bulk solution. Interestingly the cavitation threshold is dependant on the external

applied pressure: experiments using a platinum microelectrode and the aqueous $\text{Ru}(\text{NH}_3)_6^{2+/3+}$ couple in a special high pressure cell showed a linear dependence of the power required for the onset of cavitation between 1 and 20 bar [45].

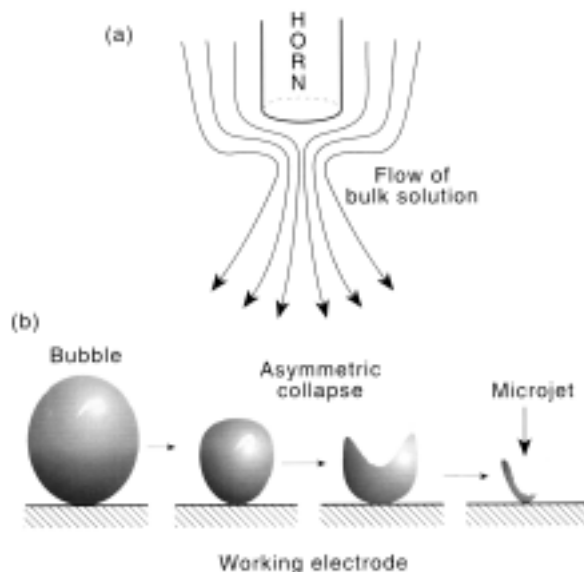


Figure 6. Representation of acoustic streaming and bubble collapse at an electrode surface

Microelectrodes can provide significant insights into the nature of cavitation and of bubble dynamics in particular [34,46–52]. Figure 7 shows a current-time curves measured at a 29 μm diameter platinum microelectrode for the $\text{Fe}(\text{CN})_6^{3-/4-}$ couple in aqueous solution under 20 kHz insonation. The current is monitored at a fixed potential corresponding to transport limited electrolysis. Note the time scale is measured in micro seconds; accordingly a special fast potentiostat design [53–60] is essential to avoid distortion that would arise with slower equipment, such as sold commercially. Examination of Figure 7 reveals spikes superimposed on a steady background, and these are attributable to bubble formation at the electrode surface. The spikes can be as high as 200 times greater than the steady-state transport limited current under silent conditions. Different types of ‘spikes’ are evident. These signals range from 50 microseconds up to a few milliseconds, spanning the range of transient cavitation (one acoustic cycle) through to stable cavitation (many acoustic cycles). Some of the spikes are periodic with frequencies of 10 or 20 kHz. Higher harmonics of the driving force can also be observed [52].

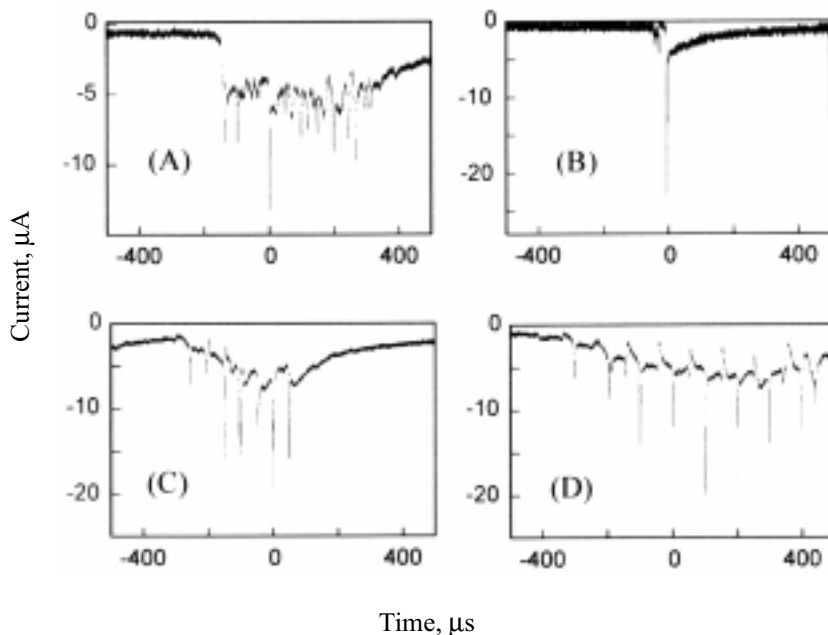


Figure 7. Chronoamperometric currents observed for the reduction of $50 \text{ mmol L}^{-1} \text{ K}_3\text{Fe}(\text{CN})_6$ in $0.1 \text{ mol L}^{-1} \text{ KNO}_3$ on a $29 \text{ }\mu\text{m}$ platinum electrode (diameter) under insonation (8.9 W cm^{-2}). Horn-to-electrode distance: 1 cm (a,c,d) or 1.5 mm (b). Figures (c), (a), and (d) are different transients obtained under the same conditions

The background current on which the spikes are superimposed is significantly greater than the spherical diffusion limited current seen under silent conditions. Moreover for electrode diameters in the range 25 to 400 microns the current was found to scale with the electrode area rather than the radius indicating a switch from convergent diffusion under silent conditions to a near uniform mass transport regime under insonation. This can be attributed to the effectiveness of acoustic streaming in delivering a very strong convective flow of material to the electrode. Application of a simple Nernst diffusion model to the data suggested, for example, that a 29 micron diameter microelectrode behaves under insonation (10 W cm^{-2}) as a uniformly accessible electrode with a diffusion layer thickness of just $8 \text{ }\mu\text{m}$ [52].

Microelectrode arrays can be used to 'size' bubbles. Figure 8 shows an array of five microelectrodes ($29 \text{ }\mu\text{m}$ in diameter) each of which can be independently and simultaneously addressed. It is thus possible to correlate signals seen on different electrodes.

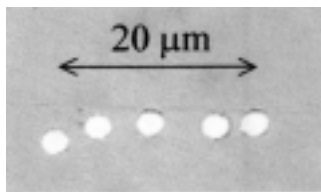


Figure 8. An array of five microelectrodes sealed in epoxy (each are 29 μm in diameter)

Figure 9 shows chronoamperometric data recorded simultaneously on the outer two and inner most electrodes for a solution containing 50 mM potassium ferricyanide in 0.1 mol L⁻¹ KNO₃ with each electrode held at a potential corresponding to the transport limited reduction to ferrocyanide.

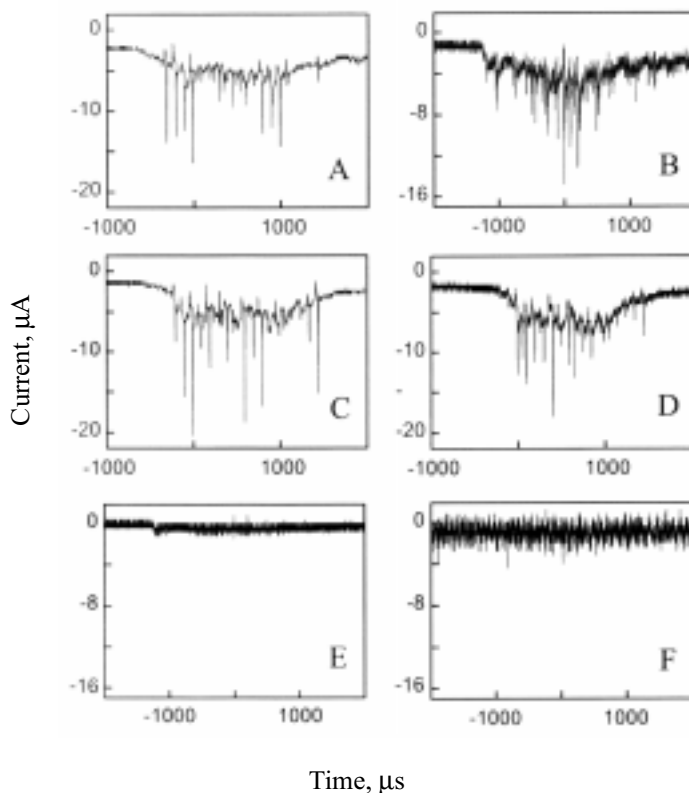


Figure 9. Chronoamperometric current recorded simultaneously (a, b and c or d, e and f) on three electrodes (diameter 29 μm) under 8.9 W cm⁻² insonation, using 50 mmol L⁻¹ K₃Fe(CN)₆ in 0.1 mol L⁻¹ KNO₃. Horn-to-electrode distance: 1 cm. Inter-electrode distance: 104 μm (a,b, and c) or less than 5 μm (d,e, and f)

A 1 cm electrode to horn separation was employed with an ultrasound power of 8.9 W cm^{-2} . Figures 9 (a) (b) and (c) correspond to interelectrode distances of $104 \mu\text{m}$ whereas for figures 9 (d) (e) and (f) the corresponding separations are no more than $5 \mu\text{m}$. In the first case there is a strong correlation of the cavitation activity from the electrode to electrode whereas in the second group the signal seen on the central electrode is voltammetrically invisible on the two electrodes just $5 \mu\text{m}$ away! One must conclude that a very wide range of bubble sizes – between 0 and $400 \mu\text{m}$ – can be present at the interface. Moreover examination of the magnitudes of the cavitation currents seen on all of the chronoamperometric currents (Figures 7 and 9) show that these are essentially of the same order of magnitude. Accordingly we believe that the microjetting, photographed by Crum [61] at 60 Hz, and shown schematically in Figure 6 is unlikely to be responsible for the underlining majority of cavitation signals seen electrochemically at the frequencies of power ultrasound since, if micro jetting were dominant, very different signals would be seen if the microelectrode was located beneath the jet, outside of the jet but within the bubble, or outside of the cavity [49,52].

Regardless of the origin of the cavitation spikes, the effectiveness of ultrasound in cleaning and even ablating surfaces is well-known [51]. For example Figure 10 shows atomic force microscopy images, taken *ex situ*, of a polished platinum electrode initially unexposed to ultrasound and after 600 s of irradiation (60 W cm^{-2}) from a horn positioned 10 mm above the electrode surface [6,62].

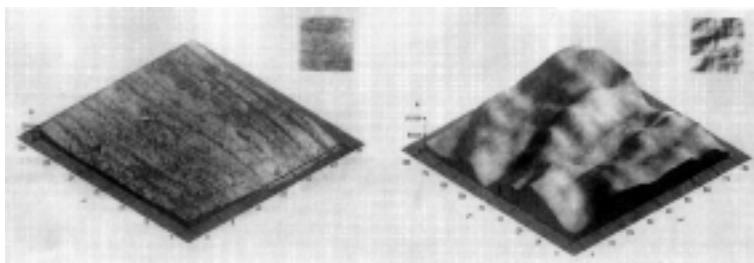
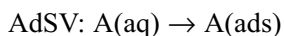
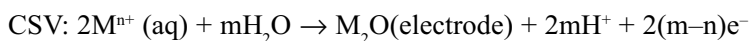
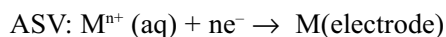


Figure 10. AFM images of a polished platinum electrode (left hand side) and after 300 s of irradiation (60 W cm^{-2}) using a horn to electrode distance of 30 mm (right hand side)

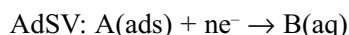
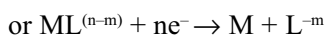
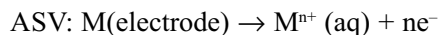
The polished electrode is rough at the $0.25 \mu\text{m}$ scale reflecting the size of the diamond paste used to polish the surface whilst after insonation significant surface ablation is evident and the corresponding roughness is *ca* $1\text{--}2 \mu\text{m}$. Further evidence for the effectiveness for ultrasound in ablating even the strongest material can be seen if the tip of an ultrasonic horn usually made from a robust titanium alloy is inspected after some hours of heavy usage. The surface has become pitted and roughened and in due course the efficiency of ultrasound transmission will be reduced.

Given the ability of ultrasound to ablate, or at lower power efficiently clean solid surfaces, we have proposed the contribution of insonation and electrochemistry in the same experiment with the aim of producing a 'self-cleaning electrode'. Figure 3 shows that this can happen either *via* a face on arrangement or as a sonotrode. In particular we have suggested that this approach – sonovoltammetry – might be most usefully applied in electroanalysis, although applications in electrosynthesis are emerging [63–69].

Stripping voltammetry is familiar [70] as a highly sensitive method for the detection of a wide range of metals and organic substances with competitively low detection limits *ca* 10^{-10} mol dm⁻³ in favourable cases. Stripping voltammetry takes three variations: anodic stripping voltammetry (ASV) (or inverse voltammetry), cathodic stripping voltammetry (CSV) or adsorptive stripping voltammetry (AdSV). In all cases there is a preconcentration step:



followed, after a suitable build up of the target material by a stripping step:



The stripping voltammetric methods show good accuracy and reproducibility with ease of computerisation and automation of analytical procedures, utilising instrumentation which is relatively simple and therefore low priced in comparison to alternatives. Nevertheless, despite extensive work with 'model systems' it is a fair observation that major real world analytical usage of voltammetric methodology has yet to realise its full potential. The limitations of this approach are recognised as largely deriving from the fact that in many target systems encountered outside of the research laboratory the inevitable presence of surface-active materials/impurities can lead to significant interferences and electrode passivation problems. These in turn dictate the need for time-consuming substrate pretreatments leading to the methodology being unattractively slow. A further limitation of the ASV method is that it is traditionally

largely dependant on the use of mercury electrodes which are seen as increasingly unattractive in the light of environmental considerations [71].

We have proposed the use of ultrasound in conjugation with stripping voltammetry [72] to enable in situ depassivation as well as opening up the possibility of a wider use of solid electrodes. The scope of the method can be illustrated with reference to the detection of copper within industrial effluent [73]. A typical sample has a pH of 2.1, a COD of 1963 mg L⁻¹, 22.6 ppm pesticide, 6.7 ppm herbicide, methanol, xylene and trace acetone in an aqueous medium. The copper was detected without sample pre-treatment; the effluent was simply diluted with 0.1 mol L⁻¹ HClO₄ and 1 mol L⁻¹ KCl. Figure 11 shows the linear sweep stripping voltammogram after 30 s conventional 'silent' deposition at a bare glassy carbon electrode. It can be seen that no stripping signal is evident. In contrast if ultrasound is applied during the stripping step, a large response becomes visible.

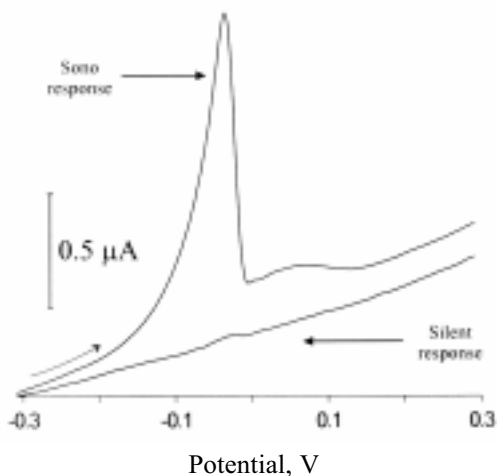


Figure 11. Linear sweep voltammograms for the copper stripping responses at a glassy carbon electrode after ultrasonically enhanced deposition and after conventional deposition (30 s deposition, 50 mVs⁻¹ scan rate)

Two peaks are apparent and if KCl is added beyond a threshold value these stabilise in size as shown in Figure 12. Under these conditions the peaks can be used analytically via the method of standard additions; Figure 13 shows the outcome and typical results are compiled in Table 1.

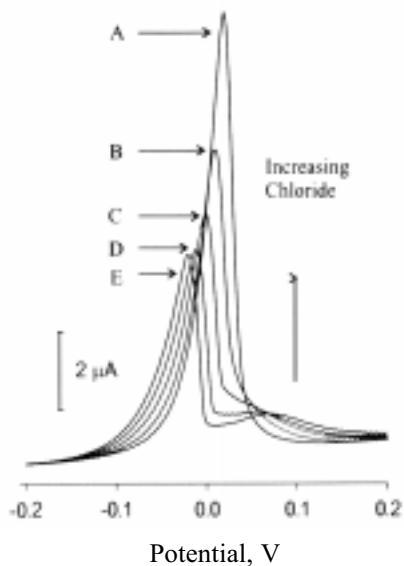


Figure 12. The influence of increasing KCl concentrations on the ASV of 6 μM copper using a 30 s sonodeposition and 50 mVs^{-1} scan rate on a glassy carbon electrode; where a, b, c, d, e correspond to 0, 1.7, 3.3, 5 and 6.7 mmol L^{-1} KCl concentrations respectively

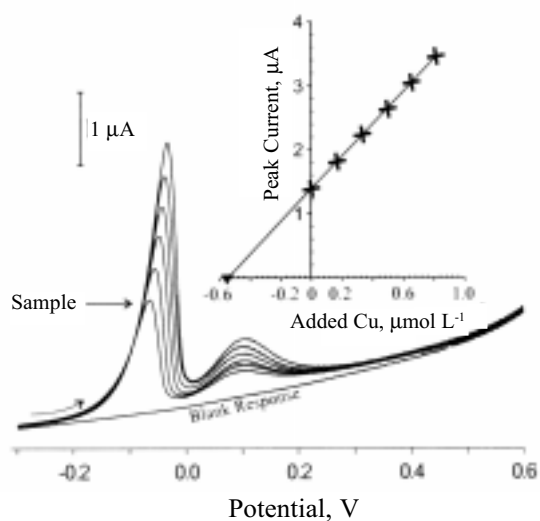


Figure 13. Standard addition calibration for the determination of copper within industrial effluent (sonodeposition time 30 s, scan rate 50 mVs^{-1})

It can be seen that not only are large signals seen under ultrasound but evidently these are quantitatively meaningful for analysis. It can be concluded that the acoustic streaming associated with insonation leads to a very large increase in the sensitivity of the ASV experiment by promoting enhances deposition and in, particular, cavitation activity on the electrode surface prevents the passivation by organic compounds that would otherwise preclude the build up of copper in the preconcentration step.

Table 1. Comparison of copper within industrial effluent samples

	Sample 1	Sample 2
	Cu, ppm	Cu, ppm
Sono ASV	2.3	8.6
Site analysis	3.0	9.0
Independent third analysis (ICP-MS)	2.5	8.1

A similar experiment can be conducted to determine copper in beer [71]. Again a glassy carbon (and so mercury free) electrode was used with sample dilution of the sample, in this using $0.1 \text{ mol L}^{-1} \text{ HNO}_3$.

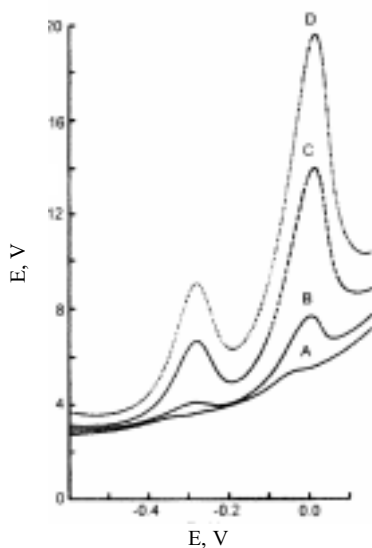


Figure 14. Square wave-ASV of aqueous solutions of beer using a 240 s deposition with a horn to electrode distance of 5mm; A) 'blank' sample, silent deposition; B) $48 \mu\text{g L}^{-1}$ standard addition of copper, silent deposition; C) $143 \mu\text{g L}^{-1}$ standard addition of copper insonated deposition (200 W cm^{-2}); D) $191 \mu\text{g L}^{-1}$ standard addition of copper insonated deposition (200 W cm^{-2})

Figure 14 again shows the copper to voltammetrically immiscible under silent condition whereas under ultrasound again *in situ* cleaning and enhanced sensitivity produce large signals, which are analytically meaningful. Typical sono-ASV determinations of copper in beer give values of $222 \pm 31 \mu\text{g L}^{-1}$ and $139 \pm 4 \mu\text{g L}^{-1}$ in different sample. Independent, blind analysis gave corresponding values of 230 and 140 respectively.

The above two examples illustrate the power of ultrasound for the *in situ* activation/cleaning of electrode surfaces: the concept can be emphasized further by an experiment in which an egg [74] is ultrasonically homogenized after mixing 1:1 with aqueous 0.1 mol L^{-1} KCl. If dopamine is then added (Fig. 15) good linear sweep voltammograms can be seen at a glassy carbon electrode for concentration of dopamine as low as $20 \mu\text{mol L}^{-1}$ provided they are run under insonation.

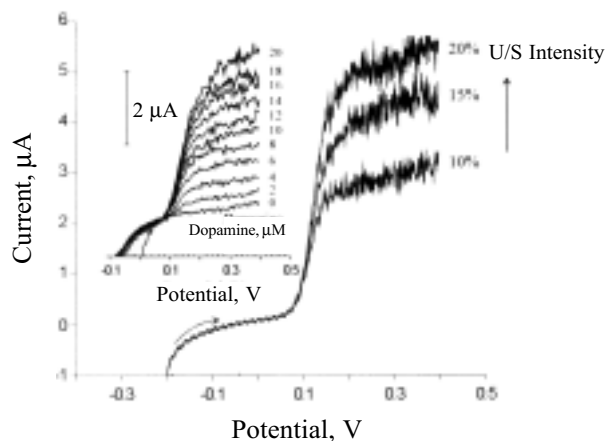
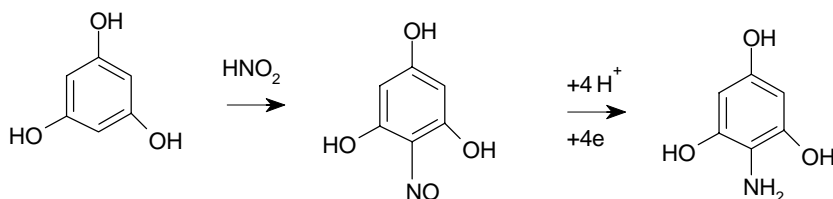


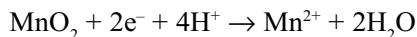
Figure 15. Sono linear sweep voltammograms for the oxidation of dopamine ($2 \mu\text{mol L}^{-1}$ aliquots) on a glassy carbon electrode. Scan rate 50 mVs^{-1}

Needless to say voltammetry in ‘scrambled egg’ under silent conditions is pointless. The approach has been used to quantify nitrite in egg [75]. A 1,3,5-trihydroxylbenzene is added to the sonicated mixture and in acid reacts with nitrite to form a nitroso compound, which is electroactive and permits the quantitative determination of nitrite in egg (Scheme 1).



Scheme 1. Electrochemical pathway for the detection of nitrite

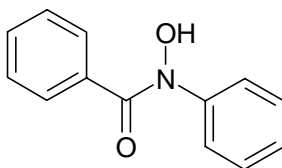
The use of new solid electrodes in sonoelectroanalysis is well illustrated by the CSV detection of manganese or lead using boron-doped diamond electrodes. The latter are diamond in which *ca.* one atom in a thousand has been replaced by boron so giving a black material with metallic conductivity where robustness makes it very attractive for sono-electroanalysis [76–87]. In addition boron-doped diamond (BDD) electrodes show an attractively wide potential window in aqueous solution [87–91] [92]. By using a high conditioning potential Mn^{2+} can be preconcentrated on a bdd electrode as MnO_2 . This allows the sono-CSV detection of manganese with a limit of detection of $1 \times 10^{-11} \text{ mol L}^{-1}$. The stripping step is:



The method has been used to determine manganese in tea [77]. Furthermore Pb^{2+} can be preconcentrated as PbO_2 on a BDD electrode [78] and has been used for the sono-CSV detection of lead in river sediments [78]. In this method the ultrasound serves also to efficiently extract the lead from the sediment (inside *ca* 30 min) as well as providing the benefits mentioned above.

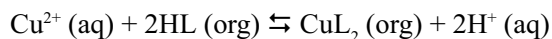
The power of ultrasound in extracting target molecules can be further illustrated with reference to the detection of copper in blood [93]. The metal ions are bound to proteins; if a sono-ASV experiment is carried out with deposition at -1.5V (*vs* SCE) on a glassy carbon electrode for a small sample of blood diluted in 0.1 mol L^{-1} nitric acid [93] the stripping signal stabilises after *ca* 1000 s of insonation prior to the sono-ASV detection. It was summarised that this led to the release of copper ions from the protein, which were thus made available for detection *via* preconcentration on the electrode surface. Levels of *ca* 500–600 $\mu\text{g L}^{-1}$ (in blood) detected were in quantitative agreement with independent analysis by atomic absorption spectroscopy.

The detection of copper in blood by the above procedure requires *ca* 2 mL of blood. A way in which this volume can be significantly reduced (to 100 μL in the case in question) is by means of biphasic sonoelectroanalysis. This exploits another feature of ultrasound, namely the ability to emulsify two immiscible liquids. Thus for example if an aqueous phase is put in contact with small amounts of insoluble organic solvent (ethyl acetate, heptane *etc.*) and ultrasound applied via a horn probe, rapid acoustic emulsification takes place [65,94,95], typically with the formation of sub-micron sized droplets of the organic phase [96–99]. If a suitable ligand is present in the organic phase, this provides a very rapid means by which target metal ions, for example, can be extracted from the aqueous phase.



Scheme 2. The ligand, N-benzoyl-N-phenylhydroxylamine used for the extraction of copper from aqueous samples

In the case of copper(II) a suitable ligand is N-phenyl,N-benzoyl hydroxylamine (Scheme 2) and a corresponding organic solvent is ethyl acetate on account of the rapid (~10 s) deemulsification after cessation of insonation:



Notice that the extraction equilibrium is pH sensitive as aqueous phase protons are released on complexation. Thus at relatively high pHs copper extraction from the aqueous phase is nearly quantitative whereas at low pH the metal can be driven from the organic solvent back into the aqueous solution.

The contact of the metal extraction *via* pH enables a double extraction approach to sono-electroanalysis [100,101]. Thus for copper in blood in the first step a dilute aqueous solution is put in contact with a small amount of ethyl acetate containing HL and acoustically emulsified so that copper(II) is transformed into the organic phase. Insonation is then stopped and the two bulk phases rapidly reform. The copper containing organic phase is then put into contact with a fresh aqueous phase but now of low pH such that the back extraction of copper is favoured. The mixture is sonicated for a short period, the phases allowed to reform and the aqueous copper containing phase used for sono-electroanalysis via sono-ASV. The merit of the double extraction is that a significant amount of surface active species will likely be removed since hydrophilic species will remain in the original aqueous phase and never be transferred to the organic phase whilst hydrophobic species will be transferred but are unlikely to be retransferred to the fresh aqueous phase [101]. Electroanalysis in the latter medium is therefore expected to be significantly easier and/or more sensitive. Measurement of copper in blood *via* this procedure were found to give quantitative results with just 100 μL corresponding to a pinprick of blood, as compared to 2 mL required for direct sonoelectroanalysis. The method has also been used for the detection of metals in fruit drinks [100].

As a final example of the sensitivity of sonoelectroanalysis we consider the detection of lead in human saliva [102] where the pertinent concentration range is *ca* 0–300 $\mu\text{g L}^{-1}$. For a relative sputum sample size of 0.2–0.5 mL used in conjugation with the

sonoelectrochemical cell shown in figure w (*ca* 35 mL) the concentration range in the analyte will be of the order of 0–10 $\mu\text{g L}^{-1}$, presenting a significant challenge to electroanalytical methods especially since the other saliva components many passivate the electrode under conventional conditions. Initially the sono-CSV approach using PbO_2 deposition was attempted, but found to lack the necessary sensitivity [103]; rather the use of mercury electrodes in the form of electroplated droplets on a glassy carbon electrode coated with a Nafion film or, for more sensitive results, without [102,104]. This is more sensitive than the PbO_2 approach since there is no requirement for the nucleation of a new separate phase, rather individual bond atoms dissolve, on reduction in to the mercury electrode. With insonation to promote the sensitivity of the ASV method, and also to activate the electrode (but using ultrasonic powers below the cavitation threshold such that mercury ablation was avoided) lead concentrations in the range 0–20 $\mu\text{g L}^{-1}$ were easily achievable [102]. The method was extended to allow for the detection of cadmium in saliva.

CONCLUSIONS

The above has shown the benefits of insonation during stripping voltammetry via the presentation of selected example. Table 2 shows a full range of real world systems that have been quantitatively addressed in this way.

Table 2. Overview of sonoelectroanalysis exemplifying the accuracy and diversity of systems studied

Analysis	Type of Voltammetry	Ultra-sound Power, (Wcm^{-2})	Tip Area, cm	Sono method	Detection Limit	Independent method	Independent method Results	Electrode Material
Lead in wine	Sono-ASV	26	1.32	$22 \pm 6 \mu\text{g L}^{-1}$	$2 \mu\text{g L}^{-1}$	AAS	$24 \pm 4 \mu\text{g L}^{-1}$ $27 \pm 4 \mu\text{g L}^{-1}$	Mercury plated platinum
Copper in beer	Sono-ASV	200	0.07	$222 \pm 31 \mu\text{g L}^{-1}$ $139 \pm 4 \mu\text{g L}^{-1}$	$32 \mu\text{g L}^{-1}$	AAS	$230 \mu\text{g L}^{-1}$ $140 \mu\text{g L}^{-1}$	Glassy Carbon
Lead in river sediment	sono-CSV	14	1.32	187.1 mg kg^{-1}	10 mg kg^{-1}	ICP-MS	206.1 mg kg^{-1}	BDD
Nitrite in egg	sono-LSV	50	0.07	$1.2 \pm 0.05 \text{ mg kg}^{-1}$ $1.4 \pm 0.05 \text{ mg kg}^{-1}$	0.045 mg kg^{-1}	MAFF Data	$1.7 \pm 0.4 \text{ mg kg}^{-1}$	Glassy carbon
Nitrate in Sewage	Sono-LSV	70	0.07	$469 \mu\text{mol L}^{-1}$		Griess Protocol	$479 \mu\text{mol L}^{-1}$	Copper modified GC

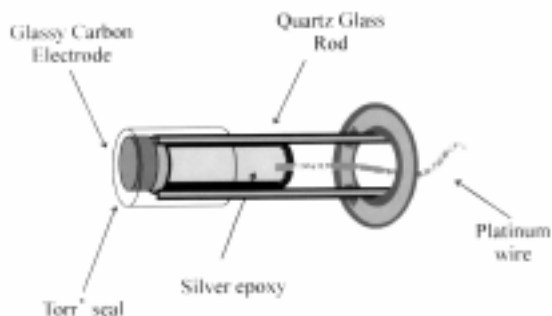
Table 2. Continuation

Lead in petrol	Sono-ASV	52	0.07	380 ± 40 mg L^{-1}		AAS	400 ± 20 mg L^{-1}	Mercury plated platinum
Manganese in instant tea	Sono-CSV	14	1.32	$1859 \mu\text{g g}^{-1}$ $914 \mu\text{g g}^{-1}$	$3 \mu\text{g g}^{-1}$	AAS	$1800 \mu\text{g g}^{-1}$ $1000 \mu\text{g g}^{-1}$	BDD
Cadmium in presence of 10ppm Triton-X	Sono-ASV	40	0.07		$0.05 \mu\text{mol L}^{-1}$	Additions of known concentration		Glassy Carbon
Lead in Lead- Copper Alloy	Sono-CSV	14	1.32		1.6 nmol L^{-1}	Additions of known concentration		BDD
Copper in blood	Sono-ASV	300	0.07	1300 ± 300 $\mu\text{g L}^{-1}$ 620 ± 60 $\mu\text{g L}^{-1}$	$90 \mu\text{g L}^{-1}$	AAS	$1300 \mu\text{g L}^{-1}$ $690 \mu\text{g L}^{-1}$	Glassy Carbon
Copper in fish gill mucous	Sono-ASV	200	0.07	$16 \mu\text{g L}^{-1}$ $21 \mu\text{g L}^{-1}$	$3 \mu\text{g L}^{-1}$	AAS	$17 \mu\text{g L}^{-1}$ $25 \mu\text{g L}^{-1}$	Mercury modified glassy carbon
Vanillin in food flavouring	Sono- biphasic	200	0.07	9.09 ± 0.21 mmol L^{-1} 9.24 ± 0.23 mmol L^{-1}	0.020 mmol L^{-1}	HPLC	9.17 mmol L^{-1} 9.30 mmol L^{-1}	Glassy Carbon
Copper in ribena®	Sono-ASV	70	0.07	45 ± 5 $\mu\text{g L}^{-1}$	$2 \mu\text{g L}^{-1}$	Std. Adn.	$45 \pm 5 \mu\text{g L}^{-1}$	Glassy Carbon
Copper in blood	Sono-ASV	70	0.07	1637 ± 26 $\mu\text{g L}^{-1}$ 1616 ± 25 $\mu\text{g L}^{-1}$	$7 \mu\text{g L}^{-1}$	Sono- ASV	1620 ± 160 $\mu\text{g L}^{-1}$	Glassy Carbon
Aqueous silver ions	Sono-ASV	14	1.32		1 mmol L^{-1}	Additions of known concentration		BDD
Copper in presence of 1000ppm SDS	Sono-ASV	70	0.07		$0.3 \mu\text{mol L}^{-1}$	% recovery from spiked sample	94.10%	Glassy Carbon
Copper in presence of 1000ppm TX-100	Sono-ASV	70	0.07		$0.3 \mu\text{mol L}^{-1}$	% recovery from spiked sample	94.00%	Glassy Carbon
5-aminosalicylic acid in tissue culture	Sono-LSV	140	0.07		$0.3 \mu\text{mol L}^{-1}$	% recovery from spiked sample	102%	Glassy Carbon
Copper in Industrial Effluent	Sono-ASV	100	0.07	2.3 ppm 8.6 ppm		ICP-MS	2.5 ppm 8.1 ppm	Glassy Carbon
Aqueous 4-chlorophenol	Sono-CV	14	1.32	unconta- minated	$1 \mu\text{mol L}^{-1}$	Additions of known concentration		BDD
Dopamine in egg homogenate	Sono-LSV	140	0.07	unconta- minated	$2 \mu\text{mol L}^{-1}$	Additions of known concentration		Mercury modified

Table 2. Continuation

Lead in Artificial Saliva	Sono-ASV	30	0.07	uncontaminated	$0.25 \mu\text{g L}^{-1}$	Additions to blank synthetic		
Lead in Human Saliva	Sono-ASV	40	0.07	$0.92 \pm 0.2 \mu\text{g L}^{-1}$ $5.10 \pm 1.0 \mu\text{g L}^{-1}$	$0.50 \mu\text{g L}^{-1}$	ICP-MS	$0.92 \pm 0.1 \mu\text{g L}^{-1}$ $4.80 \pm 0.5 \mu\text{g L}^{-1}$	Mercury modified glassy carbon
Cadmium in Human Saliva	Sono-ASV	40	0.07	$2.5 \pm 0.5 \mu\text{g L}^{-1}$ $4.9 \pm 0.05 \mu\text{g L}^{-1}$	$1 \mu\text{g L}^{-1}$	ICP-MS	$2.5 \pm 0.05 \mu\text{g L}^{-1}$ $5.0 \pm 0.05 \mu\text{g L}^{-1}$	Mercury modified glassy carbon

In almost all cases the consequence of insonation is to change a signal from a voltammetrically invisible signal to one which is large and analytically quantifiable as judged by comparison with independent methods of analysis such as ICP-MS or AAS. The change is due to acoustic streaming promoting sensitivity and, crucially, interfacial cavitation leading to in situ electrode activation in otherwise strongly passivating media. Last we note that a sonotrode is now attainable commercially [105]; Figure 16 shows the final working design based on a 3 mm glassy carbon electrode which terminates a unit acoustically compatible with widely available sonic horns.

**Figure 16.** A schematic diagram of a sonotrode

Acknowledgements

CEB thanks the EPSRC for funding a project studentship.

REFERENCES

1. Mason T.J., *Sonochemistry*, Oxford University Press, Oxford, 1999.
2. Marken F., Akkermans R.P. and Compton R.G., *J. Electroanal. Chem.*, **415**, 55, (1996).

3. Compton R.G., Eklund J.C., Marken F., Rebbitt T.O., Akkermans R.P. and Waller D.N., *Electrochimica. Acta*, **42**, 2919, (1997).
4. Eklund J.C., Marken F., Waller D.N. and Compton R.G., *Electrochimica Acta*, **41**, 1541, (1996).
5. Compton R.G., Eklund J.C., Marken F. and Waller D.N., *Electrochimica. Acta*, **41** (1996).
6. Compton R.G., Eklund J.C., Marken F., Rebbitt T.O., Akkermans R.P. and Waller D.N., *Electrochim. Acta.*, **42**, 2919, (1997).
7. Floate S., Hardcastle J.L., Cordemans E. and Compton R.G., *Analyst (Cambridge, U.K.)*, **127**, 1094, (2002).
8. Kraft A., Blaschke M. and Kreysig D., *J. Applied Electrochem.*, **32**, 597, (2002).
9. McMurray H.N., *Chem. Comm. (Cambridge, U.K.)*, **8**, 887, (1998).
10. Akkermans R.P., Ball J.C., Marken F. and Compton R.G., *Electroanalysis*, **10**, 26, (1998).
11. Horst C., Chen Y.-S., Kunz U. and Hoffmann U., *Chemical Engineering Science*, **51**, 1837, (1996).
12. Durant A., Francois H., Reisse J. and Kirsch-DeMesmaecker A., *Electrochimica Acta*, **41**, 277, (1996).
13. Arnaud G.Fr., *Demande*, **14**, (1995).
14. Koutetskii Y.A. and Levich V.G., *Doklady Akad. Nauk S.S.S.R.*, **117**, 441, (1957).
15. Levich V.G., Markin V.S. and Chirkov Y.G., *Elektrokhimiya*, **1**, 1416, (1965).
16. Ivanov Y.B. and Levich V.G., *Doklady Akad. Nauk S.S.S.R.*, **126**, 1029, (1959).
17. Koutecky J. and Levich V.G., *Zhur. Fiz. Khim.*, **32**, 1565, (1958).\
18. Lopatin V.A., Grafov B.M. and Levich V.G., **7**, 123, (1971).
19. Palade de Iribarne A., Marchiano S.L. and Arvia A.J., *Electrochim. Acta*, **15**, 1827, (1970).
20. Albery W.J., Chadwick A.T., Coles B.A. and Hampson N.A., *J. Electroanal. Chem. Interfacial Electrochem.*, **72**, 229, (1977).
21. Aoki K., Tokuda K. and Matsuda H., *J. Electroanal. Chem. Interfacial Electrochem.*, **76**, 217, (1977).
22. Aoki K., Tokuda K. and Matsuda H., *J. Electroanal. Chem. Interfacial Electrochem.*, **79**, 49, (1977).
23. Tokuda K., Aoki K. and Matsuda H., *J. Electroanal. Chem. Interfacial Electrochem.*, **80**, 211, (1977).
24. Aoki, K. and Matsuda, H., *J. Electroanal. Chem. Interfacial Electrochem.*, **90**, 333, (1978).
25. Compton R.G. and Sealy G.R., *J. Electroanal. Chem. Interfacial Electrochem.*, **145**, 35, (1983).
26. Compton R.G., Laing M.E. and Unwin P.R., *J. Electroanal. Chem. Interfacial Electrochem.*, **207**, 309, (1986).
27. Compton R.G., Pilkington M.B.G., Stearn G.M. and Unwin P.R., *J. Electroanal. Chem. Interfacial Electrochem.*, **238**, 43, (1987).
28. Compton R.G., Stearn G.M., Unwin P.R. and Barwise A.J., *J. Applied Electrochem.*, **18**, 657, (1988).
29. Booth J., Compton R.G., Cooper J.A., Dryfe R.A.W., Fisher A.C., Davies C.L. and Walters M.K., *J. Phys. Chem.*, **99**, 10942, (1995).
30. Rees N.V., Alden J.A., Dryfe R.A.W., Coles B.A. and Compton R.G., *J. Phys. Chem.*, **99**, 14813, (1995).
31. Cooper J.A. and Compton R.G., *Electroanalysis*, **10**, 141, (1998).
32. Nyborg W.L., *Proceedings of high power ultrasonics (IPC Science and Technology)*, London, England, 1972.
33. Rowe W.E. and Nyborg W.L., *J. Acoustic. Soc.*, **39**, 965, (1966).
34. Klima J., Bernard C. and DegrandC., *J. Electroanal. Chem.*, **399**, 147, (1995).
35. Banks C.E. and Compton R.G., *ChemPhysChem*, In Press, (2002).

36. Suslick K.S., Doktycz S.J. and Flint E.B., *Ultrason.*, **28**, 280, (1990).
37. Suslick K.S., Schubert P.F. and Goodale J.W., *J. Am. Chem. Soc.*, **103**, 7342, (1981).
38. Suslick K.S., Gawienowski J.J., Schubert P.F. and Wang H.H., *Ultrason.*, **22**, 33, (1984).
39. Suslick K.S., Cline R.E. Jr. and Hammerton D.A., *Ultrasonics Symposium Proceedings*, **2**, 1116, (1985).
40. Atchley A.A. and Crum L.A., *Acoustic cavitation and bubble dynamics.*, VCH, New York, N.Y, 1988.
41. Suslick K.S., *Science*, **247**, 1439, (1990).
42. Didenko Y.T., McNamara W.B.III and Suslick K.S., *J. Am. Chem. Soc.*, **121**, 5817, (1999).
43. Suslick K.S., Didenko Y., Fang M.M., Hyeon T., Kolbeck K.J., McNamara W.B.III, Mdleleni M.M. and Wong M., *Philosophical Transactions of the Royal Society of London, Series A: Mathematical, Physical and Engineering Sciences*, **357**, 335, (1999).
44. Crum L.A. and Matula T.J., *Science*, **276**, 1348, (1997).
45. Goldfarb D.L., Corti H.R., Marken F. and Compton R.G., *J. Phys. Chem. A*, **104**, 8888, (1998).
46. Birkin P.R. and Silva-Martinez S., *J. Electroanal. Chem. Interfacial Electrochem.*, **416**, 127, (1996).
47. Birkin P.R. and Silva-Martinez S., *Anal. Chem.*, **69**, 2055, (1997).
48. Birkin P.R. and Silva-Martinez S., *Chem. Comm.*, **17**, 1807, (1995).
49. Maisonhaute E., Brookes B.A. and Compton R.G., *J. Phys. Chem. B*, **106**, 3166, (2002).
50. Maisonhaute E., Javier Del Campo F. and Compton R.G., *Ultrason. Sonochem.*, **9**, 275, (2002).
51. Maisonhaute E., Prado C., White P.C. and Compton R.G., *Ultrason. Sonochem.*, **9**, 297, (2002).
52. Maisonhaute E., White P.C. and Compton R.G., *J. Phys. Chem. B*, **105**, 12087, (2001).
53. Amatore C. and Lefrou C., *J. Electroanal. Chem. Interfacial Electrochem.*, **296**, 335, (1990).
54. Amatore C., in: *Chem. React. Liq., [Proc. Int. Meet. Soc. Fr. Chim., Div. Chim. Phys.]*, 42nd (1988), 1987, p. 73.
55. Amatore C. and Lefrou C., *J. Electroanal. Chem. Interfacial Electrochemistry*, **324**, 33, (1992).
56. Amatore C. and Lefrou C., *Portugaliae Electrochimica Acta*, **9**, 311, (1991).
57. Amatore C., Bouret Y., Maisonhaute E., Goldsmith J.I. and Abruna H.D., *Chemistry – A European Journal*, **7**, 2206, (2001).
58. Amatore C., Bouret Y., Maisonhaute E., Goldsmith J.I. and Abruna H.D., *ChemPhysChem*, **2**, 130, (2001).
59. Amatore C., Maisonhaute E. and Simonneau G., *J. Electroanal. Chem. Interfacial Electrochem.*, **486**, 141, (2000).
60. Amatore C., Maisonhaute E. and Simonneau G., *Electrochem. Comm.*, **2**, 81, (2000).
61. Crum L.A., *J. Phys. (Paris)*, **11**, C8, (1979).
62. Compton R.G., Eklund J.C., Page S.D., Sanders G.H.W. and Booth J., *J. Phys. Chem.*, **98**, 12410, (1994).
63. Cintas P. and Luche J.-L., *Green Chem.*, **1**, 115, (1999).
64. Wadhawan J.D., Del Campo F.J., Compton R.G., Foord J.S., Marken F., Bull S.D., Davies S.G., Walton D.J. and Ryley S., *J. Electroanal. Chem.*, **507**, 135, (2001).
65. Wadhawan J.D., Marken F. and Compton R.G., *Pure and Appl. Chem.*, **73**, 1947, (2001).
66. Wadhawan J.D., Marken F., Compton R.G., Bull S.D. and Davies S.G., *Chem. Comm.*, **1**, 87, (2001).
67. Cognet P., Wilhelm A.-M., Delmas H., Lyazidi H.A. and Fabre P.-L., *Ultrason. Sonochem.*, **7**, 163, (2000).
68. Akkermans R.P., Roberts S.L. and Compton R.G., *Chem. Comm.*, **12**, 1115, (1999).

69. Marken F., Compton R.G., Davies S.G., Bull S.D., Thiemann T., Luisa Sa e Melo M., Neves A.C., Castillo J., Jung C.G. and Fontana A., *J. Chem. Soc., Perkin Transactions 2: Phys.Org. Chem.*, **10**, 2055, (1997).
70. Barendrecht E., *Electrochemical synthesis.*, **67**, 14, (1971).
71. Agra-Gutierrez C., Hardcastle J.L., Ball J.C. and Compton R.G., *Analyst (Cambridge, U.K.)*, **124**, 1053, (1999).
72. Marken F., Rebbitt T.O. and Compton R.G., *Electroanalysis*, **9**, 19, (1997).
73. Davis J., Cardosi M.F., Brown I., Hetheridge M.J. and Compton R.G., *Anal. Lett.*, **34**, 2375, (2001).
74. Beckett E.L., Lawrence N.S., Tsai Y.C., Davis J. and Compton R.G., *J. Pharm. Biomed. Anal.*, **25**, 995, (2001).
75. Davis J. and Compton R.G., *Anal. Chim. Acta*, **404**, 241, (2000).
76. Holt K.B., Sabin G., Compton R.G., Foord J.S. and Marken F., *Electroanalysis*, **14**, 797, (2002).
77. Saterlay A.J., Foord J.S. and Compton R.G., *Analyst (Cambridge, U.K.)*, **124**, 1791, (1999).
78. Saterlay A.J., Agra-Gutierrez C., Taylor M.P., Marken F. and Compton R.G., *Electroanalysis*, **11**, 1083, (1999).
79. Goeting C.H., Foord J.S., Marken F. and Compton R.G., *Diamond and Related Materials*, **8**, 824, (1999).
80. Saterlay A.J., Wilkins S.J. and Compton R.G., *Green Chem.*, **3**, 149, (2001).
81. Compton R.G., Marken F., Goeting C.H., McKeown R.A.J., Foord J.S., Scarsbrook G., Sussmann R.S. and Whitehead A.J.S., *Chem. Comm.*, **18**, 1961, (1998).
82. Saterlay A.J., Wilkins S.J., Holt K.B., Foord J.S., Compton R.G. and Marken F., *J. Electrochem. Soc.*, **148**, E66, (2001).
83. Saterlay A.J., Marken F., Foord J.S. and Compton R.G., *Talanta*, **53**, 403, (2000).
84. Hyde M., Saterlay A.J., Wilkins S.J., Foord J.S., Compton R.G. and Marken F., *J. Solid State Chem.*, **6**, 183, (2002).
85. Saterlay A.J., Foord J.S. and Compton R.G., *Electroanalysis*, **13**, 1065, (2001).
86. Saterlay A.J., Tibbetts D.F. and Compton R.G., *Anal. Sci.*, **16**, 1055, (2000).
87. Goeting C.H., Marken F., Gutierrez-Sosa A., Compton R.G. and Foord J.F., *New Diamond and Frontier Carbon Tech.*, **9**, 207, (1999).
88. Pleskov Y.V., Evstefeeva Y.E., Krotova M.D. and Laptev A.V., *Electrochim. Acta*, **44**, 3361, (1999).
89. C. Levy-Clement, Zenia F., Ndao N.A. and Deneuille A., *New Diamond and Frontier Carbon Technol.*, **9**, 189, (1999).
90. Panizza M., Duo I., Michaud P.A., Cerisola G. and Comninellis C., *Electrochem. Solid-State Lett.*, **3**, 429, (2000).
91. J. Xu M.C.G., Q. Chen J., Strojek W., Lister T.E. and Swain G.M., *Anal. Chem.*, **69**, 591A, (1997).
92. Manivannan A., Tryk D.A. and Fujishima A., *Electrochem. Solid-State Lett.*, **2**, 455, (1999).
93. Hardcastle J.L., Murcott G.G. and Compton R.G., *Electroanalysis*, **12**, 559, (2000).
94. Banks C.E., Rees N.V. and Compton R.G., *J. Electroanal. Chem.*, **535**, 41, (2002).
95. Wain A.J., Lawrence N.S., Davis J. and Compton R.G., *Analyst (Cambridge, U.K.)*, **127**, 8, (2002).
96. Behrend O., Ax K. and Schubert H., *Ultrason. Sonochem.*, **7**, 77, (2000).
97. Behrend O. and Schubert H., *Ultrason. Sonochem.*, **8**, 271, (2001).
98. Banks C.E., Klymenko O.V. and Compton R.G., *PhysChemChemPhys*, **5**, 1652 (2003).
99. Marken F., Compton R.G., Bull S.D. and Davies S.G., *Chem. Comm. (Cambridge, U.K.)*, **11**, 995, (1997).
100. Hardcastle J.L. and Compton R.G., *Analyst (Cambridge, U.K.)*, **126**, 2025, (2001).
101. Hardcastle J.L. and Compton R.G., *Electroanalysis*, **14**, 753, (2002).
102. Hardcastle J.L., West C.E. and Compton R.G., *Analyst (Cambridge, U.K.)*, **127**, 1495, (2002).

103. Hardcastle J.L., Thesis: Sonoelectroanalysis-Oxford University, Oxford, 2002.
104. West C.E., Hardcastle J.L. and Compton R.G., *Electroanalysis*, **14**, 1470, (2002).
105. http://windsor-ltd.co.uk/products/sensors/sensor_sonotrodepage.asp.

Received December 2002

Accepted March 2003